Article

Effect of graphite powder on thermal behavior of phase change material

Makoto Shibahara[1],*, Yuuhi Hatta[1], Qiusheng Liu[1], Sutopo Purwono Fitri[2]

[1] Graduate School of Maritime Sciences, Kobe University, Kobe 658-0022, Japan

[2] Marine Engineering Department, Sepuluh Nopember Institute of Technology, ITS Campus Sukolilo, Surabaya 60111, Indonesia

* Corresponding author: Makoto Shibahara, sibahara@maritime.kobe-u.ac.jp

Abstract: The effect of graphite powder on the thermal behavior of phase change material (PCM) was investigated experimentally. It is well known that the graphite is contributed to enhance the thermal response. However, the effect of graphite on the supercooling of the PCM is not clear when a highly heat conductive material is added. In this study, the specific heat of the PCM based on sugar alcohol such as D-mannitol and inositol was measured with an adiabatic scanning calorimeter. The enthalpy and entropy during the phase-change process were obtained by the measured specific heat of the PCM. Additionally, the exergy analysis was conducted to evaluate the thermal energy storage of PCM. As the experimental results, the specific heat of D-mannitol during the phase change process was higher than that of inositol. Moreover, it was found that the addition of graphite powder at the mass fraction of 9% improves the thermal behavior of D-mannitol with lower supercooling while maintaining latent heat. The suppression of supercooling by the addition of 9% graphite powder was 37.5%.

Keywords: phase change material; latent heat; thermal response; graphite powder; supercooling

1. Introduction

To address the issues of global warming, the utilization of waste heat has been considered in maritime industries. For effectively utilizing waste heat, the organic Rankine cycle (ORC), which generates power by exhaust heat recovery, is highly attractive. There is a need for heat recovery technologies utilizing the ORC with latent-heat storage materials, and it is important to understand the thermal properties (specific heat, latent heat, etc.) of these materials for the efficient operation of heat recovery systems [1].

Bo et al. [2] investigated the thermal properties of tetradecane, hexadecane, and their binary mixtures using differential scanning calorimetry (DSC). They concluded that binary mixtures are promising candidates for use as phase change materials (PCMs) in cooling systems. Hidaka et al. [3] evaluated the fundamental properties of D-threitol, an optical isomer of erythritol. The results showed that threitol has a heat storage density that is nearly equivalent to ice, with a total heat capacity of 313 kJ/kg in the operating temperature range of 353 to 373 K. It was also revealed that threitol exhibits significant supercooling. Kageyama et al. [4] investigated the relationship between the solidification rate of erythritol and the characteristics of the heat transfer tube surface. They revealed that as the numerical value of the average roughness of the heat transfer tube surface increases, the solidification rate of erythritol decreases, indicating a tendency for thermal conductivity to decrease. Shibahara et al. [5] investigated the thermal characteristics of sodium acetate trihydrate and D-mannitol, using thermogravimetry and differential thermal analysis (TG-DTA). The

experimental result of sodium acetate trihydrate showed that the supercooling of D-mannitol was lower than that of sodium acetate trihydrate. Yan et al. [6] suggested that heterogeneous nucleation could suppress supercooling of hydrate salts [7]. They experimentally investigated the effects of several additives on calcium chloride hexahydrate. When mixing graphite, iron oxide III, potassium chloride (KCl), and strontium chloride hexahydrate (SrCl$_2$6H$_2$O) at 1/3/5 wt.% ratio, they found that strontium chloride hexahydrate at 3 wt.% yielded optimal results. While the latent heat capacity decreases linearly and proportionally with the addition ratio, it does not necessarily follow the same trend in terms of supercooling suppression.

The melting process of D-mannitol was clarified by numerical simulation [8]. They also measured the transient heat-transfer coefficient of D-mannitol under natural convection to develop a heat exchanger for latent-heat storage materials [9]. Mojiri et al. [10] developed the macro-scale thermal energy system using D-mannitol. Karthikeyan et al. [11] carried out the commercial computational fluid dynamics (CFD) analysis to observe the transient melting behavior of D-mannitol. They conducted melting simulations by modeling D-mannitol within stainless steel spheres with diameters of 80 mm and 40 mm and applying heat. The simulation results indicated that the unmelted portions tended to fragment into smaller pieces as the melting of mannitol progressed. These latent heat storage materials, especially those operating in the medium-to-low temperature range, have a critical issue of possessing low thermal conductivity, which significantly impacts the efficiency of waste heat recovery cycles.

In order to overcome the low thermal conductivity of the PCMs, high thermal conductive PCMs have been developed by adding the expanded graphite [12]. Bai et al. [13] measured the temperature of composed PCM with the expanded graphite at the different light intensity. They showed that the thermal response of the PCM improved by adding the expanded graphite of 10% at the irradiation intensity of 0.2 W/m^2. Although there are many studies on the thermal properties of latent heat storage materials, the supercooling is also not discussed when a highly heat conductive graphite powder was added to the PCM. Since the supercooling observed in latent heat storage materials, it is crucial to control supercooling of the PCM.

In this study, the latent heat capacities of latent-heat storage materials were investigated using an adiabatic scanning calorimeter, and experiments related to heat-response characteristics were conducted to improve thermal responsiveness and to suppress supercooling with graphite additions.

2. Material and methods

In this experiment, three types of sugar alcohol with high latent heat and excellent corrosion resistance were investigated: D-mannitol (melting point: 439 K), inositol (498 K), and sorbitol (367 K) [14]. **Figure 1** presents a graph comparing major PCMs and their latent heat capacities [5]. Among various substances, including organic materials and hydrated salts, sugar alcohols exhibit a relatively high latent-heat capacity and possess the distinctive feature of having melting points concentrated in the medium temperature range of 373 K to 573 K. Sugar alcohols also have additional

advantages, including consistent heat absorption and release, high heat-storage capacity per unit volume, chemical stability and low corrosivity, and low cost.
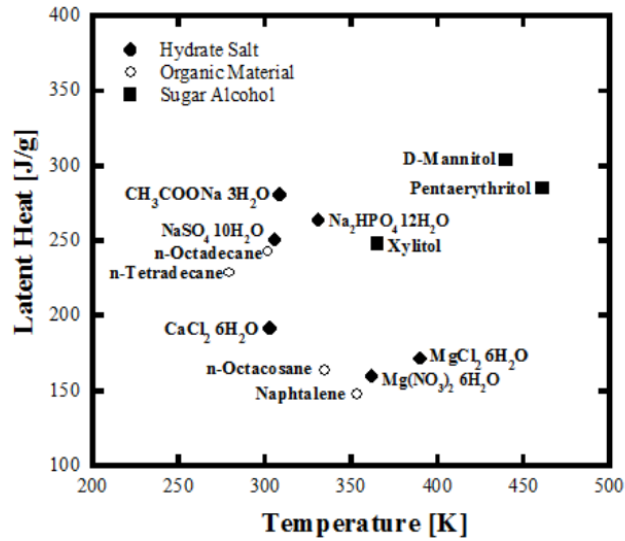

Figure 1. Relationship between the latent heat of PCMs and the melting temperature [5].

Figure 2 shows a schematic representation of the interior of the adiabatic scanning calorimeter (Shinkuuriko, SH-3000-M). The measurement accuracy of specific heat is ±3.0%. Within the chamber, vial containers containing the samples were placed, and the temperature history of the phase transition process was recorded using a data logger while heating, and the temperature increased with an electric furnace. The powdered samples (0.180 g each) were placed in heat-resistant vials. They were then stirred for 30 s using a stirrer. Subsequently, the samples were heated in the furnace of the adiabatic scanning calorimeter at a rate of 0.8 J/s. Heating continued until the samples transitioned from the solid to the liquid phase. The material's temperature was recorded using a data logger. The specific heat of the samples was calculated from the obtained temperature changes and the elapsed time using the following equation:

$$C_p = \frac{Q \cdot \Delta\tau}{M \cdot \Delta T} - \frac{M' C_p{}'}{M} \tag{1}$$

where, C_p (J/g·K), Q (W), M (g), ΔT (K), $\Delta\tau$ (s), and $M'C_p{}'$ (J/g·K) represent the specific heat, power, mass, temperature rise, elapsed time, and heat capacity of the vial, respectively.
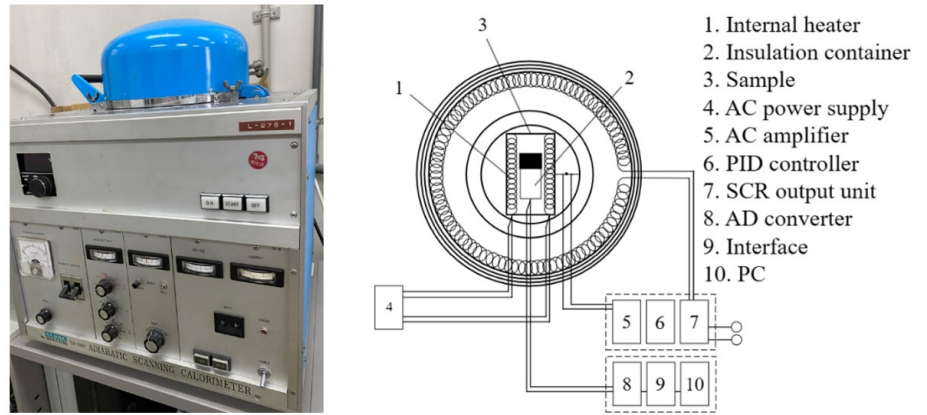
Figure 2. Adiabatic scanning calorimeter.

M'C_p' was determined in advance through a blank test. The latent heat was calculated from the change in enthalpy by using the following equation based on the relationship between the specific heat obtained from Equation (1) and temperature. The difference in enthalpy during the phase transition from solid to liquid was considered as the latent heat:

$$\Delta h = \int_{T_1}^{T_2} C_p \, dT \tag{2}$$

where, Δh (J/g), T_1 (K), and T_2 (K) are the enthalpy change, reference temperature, arbitrary temperature, respectively. Furthermore, the heat stored during the phase transition was determined from Equation (2), and an exergy analysis was conducted using Equation (3) [15].

$$\Delta e = \Delta h - T_0 \Delta s \tag{3}$$

where, Δs was the entropy calculated by Equation (4). T_0 (K) is the ambient temperature, which was set to 293 K in this study.

$$\Delta s = \int_{T_1}^{T_2} \frac{C_p}{T} dT = C_p \ln \frac{T_2}{T_1} \tag{4}$$

where, C_p is the measured specific heat from Equation (1).

In addition to this, we also conducted experiments to improve the thermal responsiveness of latent-heat storage materials. A highly conductive graphite powder was added to mannitol to enhance its thermal responsiveness; this addresses a common challenge in PCMs at moderate to low temperatures. **Figure 3** displays a schematic diagram of the experimental setup. The experimental procedure is as follows:

1) D-mannitol (Fujifilm Wako Pure Chemical Corporation, Osaka, Japan) and graphite powder (AS-One, Osaka, Japan) with average particle sizes ranging from 5 to 11 mm were weighed using a digital scale (A&D HT-120) and mixed for a specified duration using a vortex mixer.

2) A heater was set in a test tube, and the mixture from step (1) was placed inside.

3) The test tube was inserted into a container with rubber stoppers on the top and bottom, sealed, and evacuated to approximately 66 kPa.

4) A thermocouple was inserted to a specified depth.

5) Initial heating was performed once using the heater, and measurements were taken from the second heating cycle after the material had melted and solidified.

The experiments of thermal response were conducted in this sequence. For a total sample mass of 11 g, six samples were prepared by varying the mixing ratio of graphite. The input heating power was adjusted to 50 W, as described in Equation (5).

$$P = VI = V \frac{V_R}{R_s} \tag{5}$$

where, P (W), V (V), I (A), V_R (V), and Rs (Ω) are heat input, voltage of volt slider, electrical current, voltage across the shunt, and shunt resistance, respectively. The temperature of the composite material was measured using a K-type thermocouple inserted into the test tube and recorded by a data logger (GRAPHTEC, GL240). Vacuum insulation was maintained at 66 kPa by a vacuum pump to prevent heat dissipation during measurements.
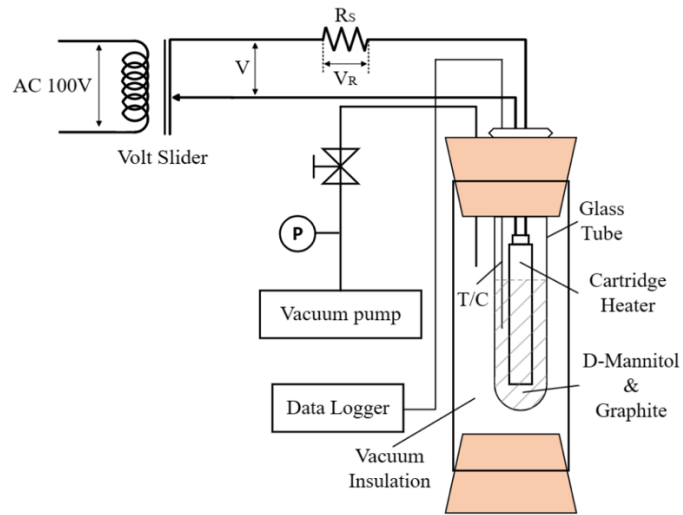

Figure 3. Experimental setup.

The uncertainty of the temperature measured by the thermocouple was estimated as follows [16]:

$$\frac{\Delta T}{T} = \sqrt{\left(\frac{\Delta T_{tc}}{T}\right)^2 + \left(\frac{\Delta T_{cj}}{T}\right)^2} \tag{6}$$

where, the uncertainties of the thermocouple, $\frac{\Delta T_{tc}}{T}$, and the cold junction, $\frac{\Delta T_{cj}}{T}$, respectively. ΔT_{tc} and ΔT_{cj} are $\pm 0.05\%$ of rdg + 1.0 K and ± 0.5 K, respectively.

3. Results and discussion

3.1. Melting point and specific heat of PCMs

Temperature-time curves for mannitol, inositol, and sorbitol are shown in **Figure 4**. The temperature of all three materials increases with a linear heating process under the solid phase up to 1000 s. Since the melting temperature of sorbitol is about 365.15 K, the temperature gradient of Sorbitol has been changed for the phase change from

solid to liquid state. Similarly, for mannitol and inositol, there is a decrease in the gradient in the temperature—time curve, indicating the onset of the melting point of the material and the start of the phase transition. After the phase transition, the gradient increases again, indicating that the material has completed the phase transition and transitioned into the latent heat (liquid phase) state. **Table 1** compares the melting points obtained in this study with the literature [14]. The measured data are in good agreement with the literature values, indicating a high accuracy of the measurement for each material.

Figures 5–7 show the relationship between the specific heat and temperature for each sample, which were calculated using Equation (1). The specific heat remains constant up to the melting temperature. Subsequently, a significant peak in specific heat appears from the onset of phase transition. It is considered that the increase of specific heat is caused by the latent heat. **Table 2** shows the average specific heat for each sample in phase intervals. It is understood that mannitol is higher average specific heat than that of sorbitol during the phase transition. In the solid phase and liquid phase, the specific heat of mannitol is higher than that of inositol.
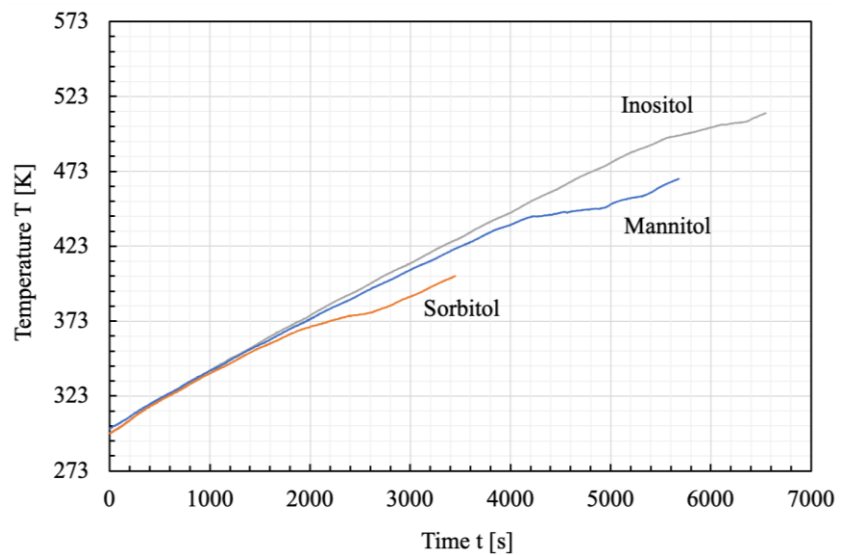

Figure 4. Relationship between the temperature and time at various materials.

Table 1. Comparison of melting temperature with literature values [14].

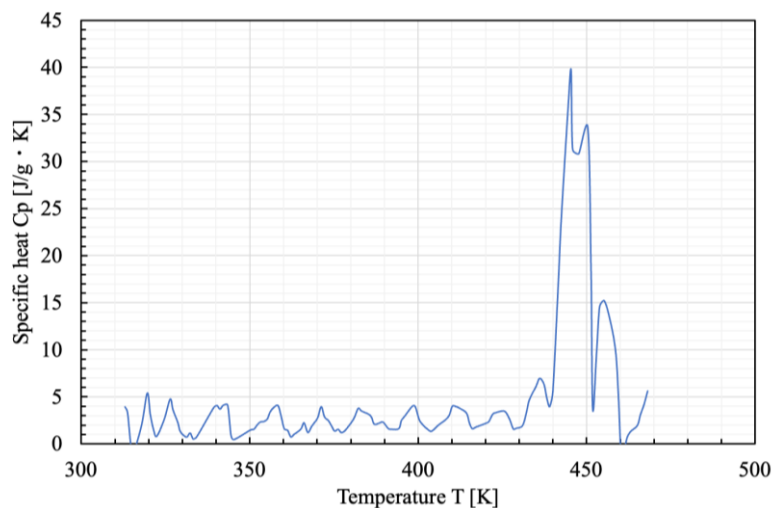| Materials	Measured value (K)	Literature value (K) [14]
Mannitol	439.05	439.35
Sorbitol	365.15	366.45
Inositol	496.05	498.65

Figure 5. Specific heat of D-mannitol.
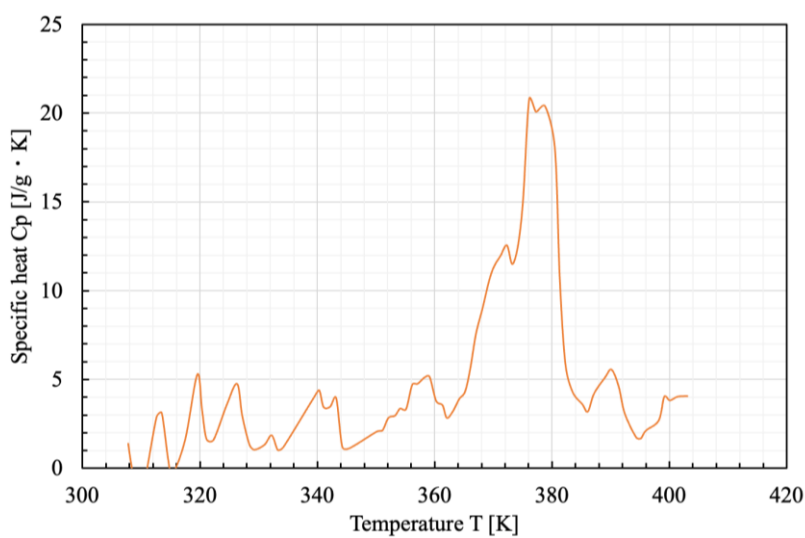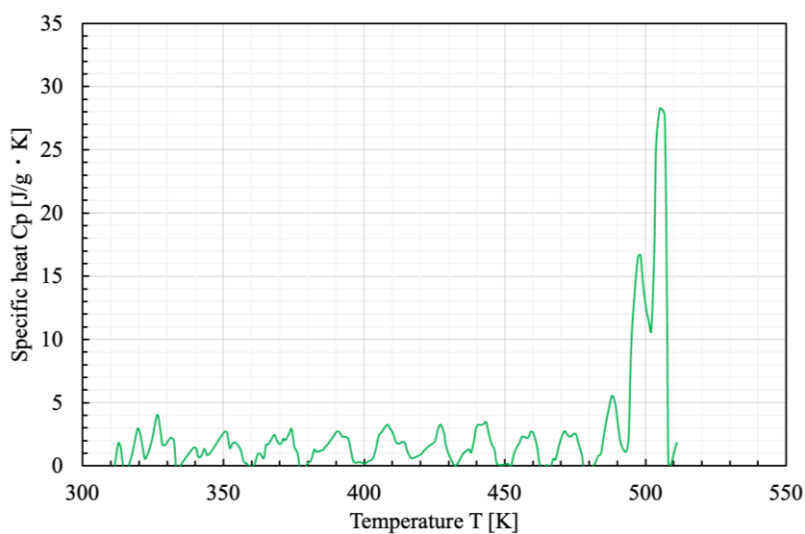

Figure 6. Specific heat of sorbitol.

Figure 7. Specific heat of inositol.

Table 2. Average specific heat for each phase.

Material	Specific heat c_p (J/g·K)		
	Solid	Solid-Liquid	Liquid
Mannitol	2.58	18.40	2.17
Sorbitol	2.49	9.93	3.58
Inositol	1.43	14.50	0.99

3.2. Enthalpy and entropy of PCMs

Figure 8 shows the enthalpy stored by each material at various temperatures, which were calculated using Equation (2). As shown in **Figure 8**, the enthalpy of mannitol shows a linear increase from approximately 350 K to 440 K. This represents the sensible heat in the solid phase. After the melting point, the enthalpy increases, indicating the latent heat during the phase transition. The comparison shows that there is a significant difference in the stored thermal energy between the solid state and during the phase change. **Table 3** compares the latent heat for each material. From this table, it is clarified that mannitol stores the largest latent heat during the phase transition, followed by inositol and sorbitol, which have nearly equivalent values.

Table 3. Comparison of latent heat.

Material	Latent heat L (J/g)
Mannitol	394.2
Sorbitol	230.6
Inositol	229.0
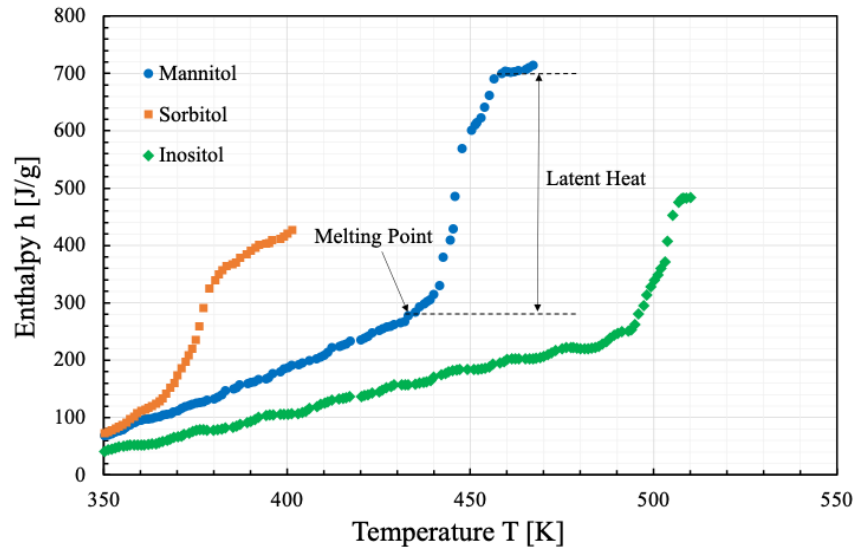
Figure 8. Enthalpy—Temperature curves.

Figures 9–11 show the entropy for each material, which were calculated using Equation (4). As shown in **Figure 9**, the entropy increases between 440 K and 460 K due to the latent heat of mannitol. For sorbitol and inositol, the entropy also increases due to the latent heat as shown in **Figures 10** and **11**. Since the latent heat of sorbitol is lower than that of mannitol, the entropy of sorbitol is also lower than that of mannitol

during the phase change. **Table 4** shows the average entropy values for each sample in the three phases. From this table, it is can be seen that the entropy of inositol has the lowest value in all phases.
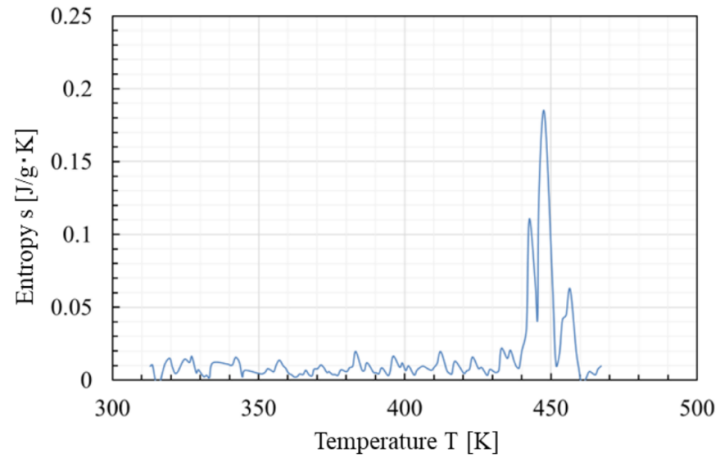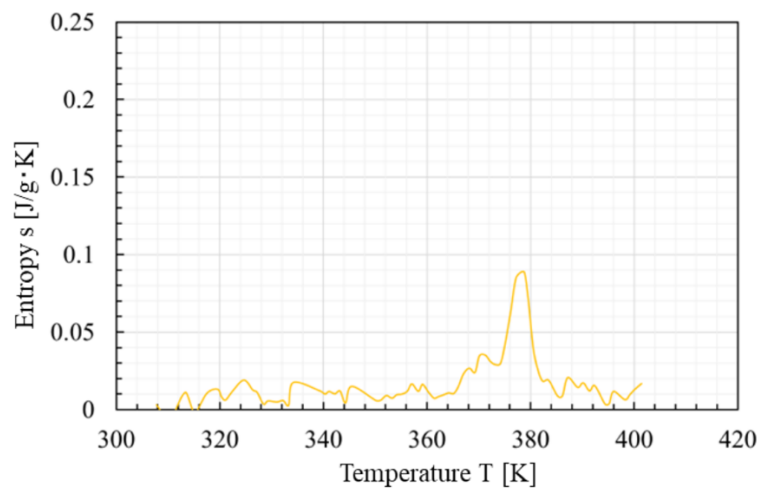
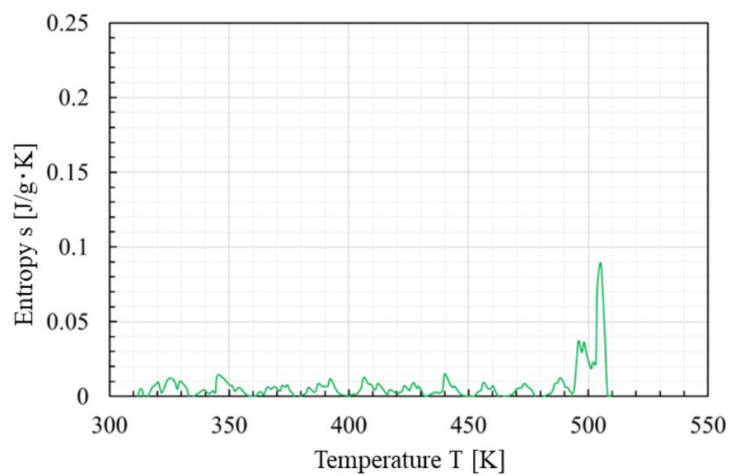**Figure 9.** Entropy of mannitol.

Figure 10. Entropy of sorbitol.

Figure 11. Entropy of inositol.

Table 4. Average entropy for each phase.

Materials	Entropy *e* (J/g·K)		
	Solid	**Solid-Liquid**	**Liquid**
Mannitol	0.008	0.049	0.004
Sorbitol	0.008	0.033	0.012
Inositol	0.004	0.029	0.001

3.3. Exergy evaluation of PCMs

Figure 12 shows the latent heat and exergy at an ambient temperature of 293 K for the measured samples. The exergy was obtained in Equation (3), which is the difference between the enthalpy integrated in Equation (2) and the entropy calculated in Equation (4). The latent heat for sorbitol, mannitol, and inositol were 230.6, 394.2, and 229.0 J/g, respectively, with mannitol indicating the highest latent heat value. Conversely, the exergy for sorbitol, mannitol, and inositol were 55.7, 136.5, and 95.5 J/g, respectively. Both the latent heat and exergy parameters substantiate mannitol's superiority as a latent-heat storage material. The values of the exergy during the phase transition and the percentage of the exergy relative to the latent heat are shown in **Table 5**. From this table, it is understood that the amount of heat extractable as work is less than 50% for all materials, and for sorbitol, approximately 75% of the heat cannot be utilized. Among these three materials, mannitol can store and extract more heat, making it an excellent heat-storage material. Therefore, in the next section, we investigate the effect of adding graphite to mannitol on its thermal responsiveness.
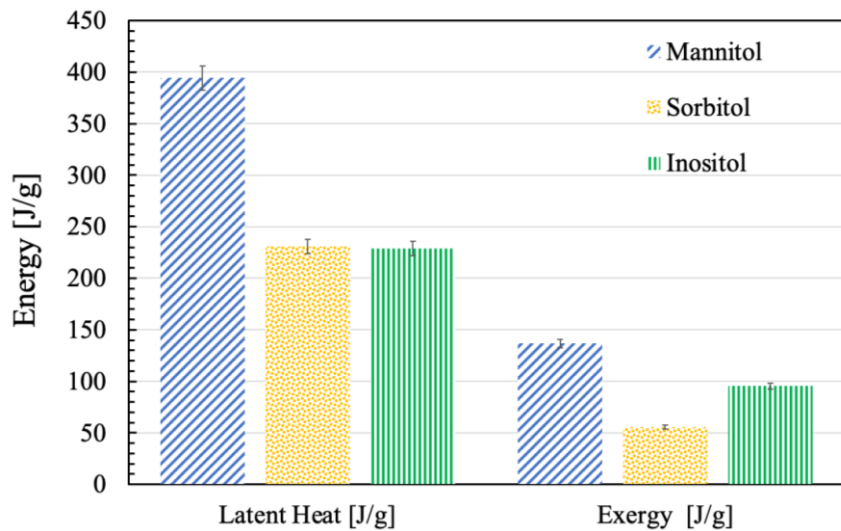
Figure 12. The latent heat and exergy evaluation of thermal storage materials.

Table 5. The exergy during the phase transition and the percentage of exergy relative to the latent heat.

Materials	Latent heat *L* (J/g)	Exergy *e* (J/g)	*e*/*L* (%)
Mannitol	394.2	136.7	34.7
Sorbitol	230.6	55.7	24.2
Inositol	229.0	95.5	41.7

3.4. Thermal responsiveness enhanced by graphite addition

Figure 13 shows the relationship between elapsed time and the temperature for mannitol with varying mass fractions of graphite powder. The temperature of pure mannitol increased with time as mentioned in **Figure 4**. As the graphite was added to the mannitol, the temperature gradient increased with graphite loading at around 500 s.

Thus, the temperature rises within the solid-phase region became faster, resulting in a shorter time to reach the melting point (439.35 K). After the phase transition, the temperature gradually increased and the heating of the heater was stopped. During cooling, the temperature of mannitol decreased rapidly, and supercooling occurs until it reaches around 423.15 K, below the melting point. As heat release due to solidification begins, the temperature rises to the original melting point, and the phase transition continues for about 400 s. Once the mannitol has transitioned to the solid phase, the temperature dropped to ambient.
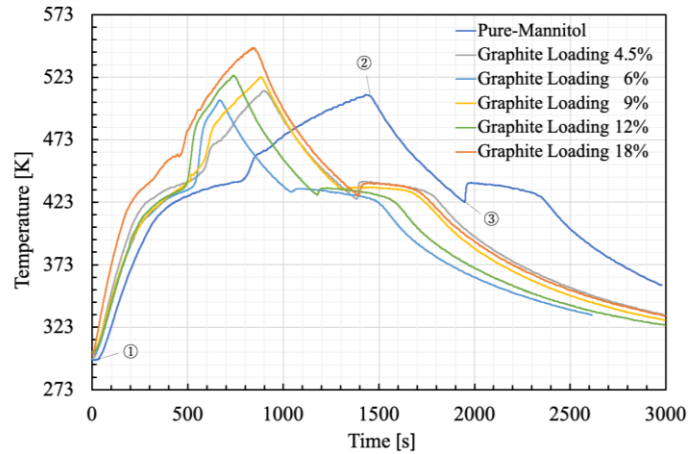

Figure 13. The effect of graphite loading on the thermal response of the PCM.

Figure 14 is an image captured from melting to solidification of pure mannitol. A series of the phase transitions can be observed in the images from left to right. It is considered that the partial melting due to natural convection occurred [8]. As the thermal stratification due to the natural convection has been developed in the PCM, the solid-liquid interface appeared as shown in **Figure 14**.
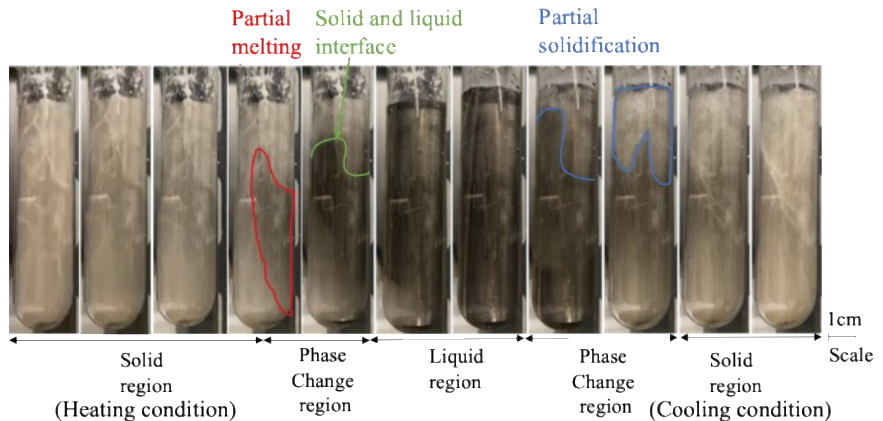

Figure 14. The phase change process of mannitol.

Figure 15 compares the dimensionless time required for pure mannitol to undergo the melting process as a reference. As the addition of graphite increases, the dimensionless time to reach the melting point becomes shorter, indicating improved thermal responsiveness. It seems that the thermal conductivity of the composite material could be enhanced by forming a complete phonon transmission channel by the addition of the graphite powder [17].
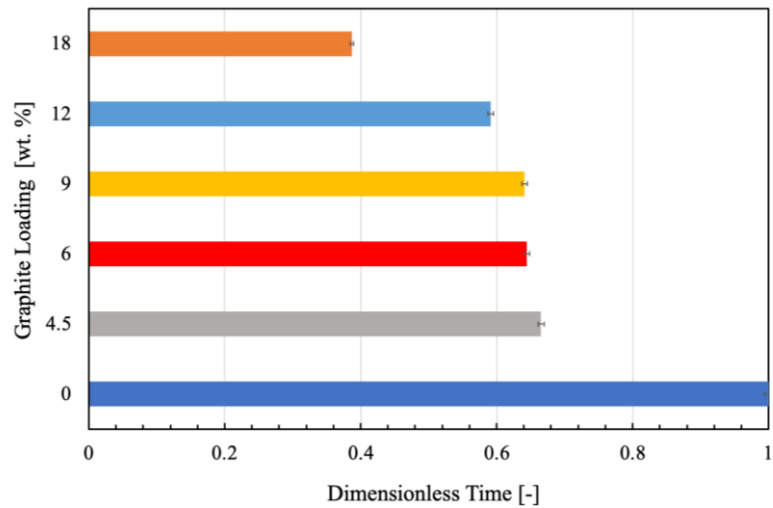

Figure 15. The dimensionless time required for phase transition.

Figure 16 illustrates the relationship between the graphite loading and the thermal energy charging. As the graphite loading increases, the stored energy decreases, indicating that graphite may penetrate between mannitol molecules, weakening the binding forces and causing such a phenomenon. In other words, as mentioned earlier, there is a trade-off between the thermal responsiveness and the thermal energy charging.
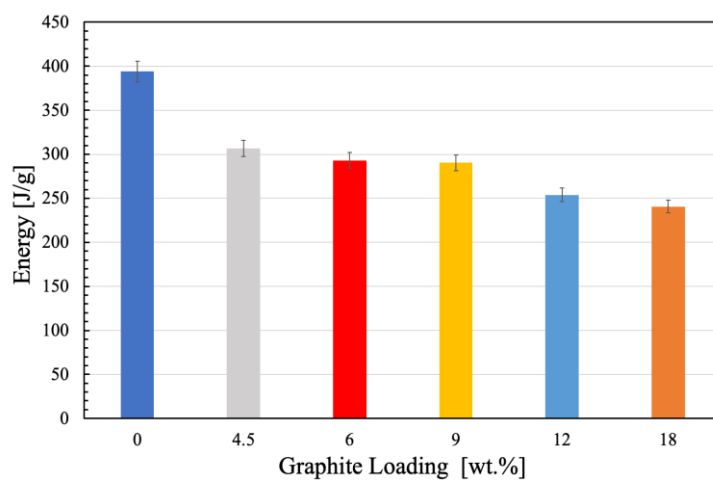

Figure 16. The relationship between the thermal energy charging and the graphite loading.

Figure 17 shows the relationship between supercooling and graphite addition. Supercooling was assessed as the difference between the melting point and the actual solidification temperature. It can be observed from this figure that the addition of

graphite reduces supercooling. The supercooling suppression by adding graphite powder of 9% was 37.5% compared to pure D-mannitol. It seems that the crystallization of D-mannitol was caused by heterogeneous nucleation on graphite surfaces, as the graphite powder was doped as the nucleation sites for crystal seeds [7,18]. Since the interfacial surface area between D-mannitol and the graphite with high thermal conductivity was expanded, it was understood that the heat conduction was improved and the crystal growth was promoted [19].
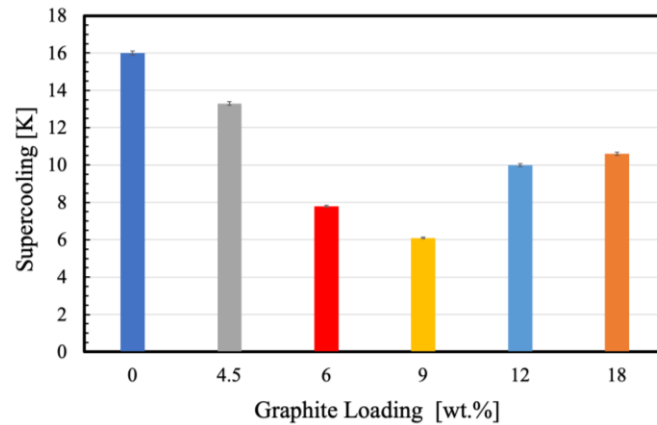

Figure 17. The relationship between supercooling and graphite loading.

4. Conclusion

The effect of adding graphite powder to D-mannitol at various mass percentages was investigated, experimentally. The key findings from this study are as follows.

- The experiments related to heat-response characteristics were conducted to improve the thermal response and to suppress supercooling with graphite additions.
- The enthalpy and entropy during the phase-change process were obtained by the measured specific heat of the PCMs.
- The specific heat of D-mannitol during the phase change process was higher than that of inositol.
- The addition of graphite powder at the mass fraction of 9% improves the thermal behavior of D-mannitol with lower supercooling while maintaining latent heat.
- The suppression of supercooling by the addition of 9% graphite powder was 37.5% compared to pure D-mannitol.

Conflict of interest: The authors declare no conflict of interest.

Nomenclature

Cp	Specific heat, J/g·K
I	Electric current, A
M	Mass, g
P	Heat input, W
Q	Power, W
R_s	Shunt resistance, Ω
T	Temperature, K
T_0	Ambient temperature, K
T_1	Reference temperature, K
T_2	Arbitrary temperature, K
V	Voltage of volt slider, V
V_R	Voltage of shunt resistance, V
$M'Cp'$	heat capacity of the vial, J/g·K
e	Exergy, J/g
h	Enthalpy, J/g
s	Entropy, J/g

Greek symbols

$\Delta\tau$	elapsed time, s

Subscripts

cj	cold junction
dl	data logger
tc	thermocouple

References

1. Alvi JZ, Feng Y, Wang Q, et al. Effect of phase change materials on the performance of direct vapor generation solar organic Rankine cycle system. Energy. 2021; 223. doi: 10.1016/j.energy.2021.120006
2. Bo H, Gustafsson EM, Setterwall F. Tetradecane and hexadecane binary mixtures as phase change materials (PCMs) for cool storage in district cooling systems. Energy. 1999; 24(12): 1015–1028.
3. Hidaka H, Yamazaki M, Yabe M, et al. Evaluation of Fundamental Characteristics of Threitol for Latent Heat Storage for Hot Water Supply. Kagaku Kogaku Ronbunshu. 2004; 30(4): 552–554.
4. Kageyama H, Hidaka H, Kubota M, et al. Study on the Initial Solidification Rate Acceleration of Erythritol Used for Latent Heat Storage. In: Proceedings of the 38th Annual Meeting on the Society of Chemical engineering; 16–18 September 2006; Fukuoka, Japan.
5. Shibahara M, Liu QS, Fukuda K. Thermal characteristics of phase change materials for waste heat recovery system. J Jpn Inst Mar Eng. 2015; 50(6): 63–70.
6. Yan L, Charles J, Romero EC, et al. Optimizing supercooling and phase stability by additives in calcium chloride hexahydrate for cyclical latent heat storage. Int Commun Heat Mass Transfer. 2023; 149. doi: 10.1016/j.icheatmasstransfer.2023.107119
7. Beaupere N, Soupremanien U, Zalewski L. Nucleation triggering methods in supercooled phase change materials (PCM), a review. Thermochim Acta. 2018; 670: 184–201.

8.   Shibahara M, Liu QS, Fukuda K. Heat transfer characteristics of D-mannitol as a phase change material for a medium thermal energy system. Heat Mass Transfer. 2016; 52: 1993–2004.

9.   Shibahara M, Liu QS, Fukuda K. Transient natural convection heat transfer of liquid D-mannitol on a horizontal cylinder. Renewable energy. 2016; 99: 971–977.

10. Mojiri A, Grbac N, Bourke B, Rosengarten G. D-mannitol for medium temperature thermal energy storage. Sol Energy Mater Sol Cells. 2018; 176: 150–156.

11. Karthikeyan S, Nagasudhan N, Nithin RA, et al. Transient numerical analysis on the melting characteristics of Paraffin and D-mannitol phase change materials for latent thermal energy storage. Mater. Today Proc. 2021; 45(7): 6306–6313.

12. Wang T, Liu Y, Meng R, Zhang M. Thermal performance of galactitol/mannitol eutectic mixture/expanded graphite composite as phase change material for thermal energy harvesting. J Energy Storage. 2021; 34. doi: 10.1016/j.est.2020.101997

13. Bai Y, Qiu W, Wang S. D-mannitol-based eutectic composite phase change materials with high thermal conductivity and solar-thermal conversion. Int J Energy Res. 2022; 46(11): 15722–15732.

14. Solé A, Neumann H, Niedermaier S, et al. Stability of sugar alcohols as PCM for thermal energy storage. Sol Energy Mater Sol Cells. 2014; 126: 125–134.

15. Jegadheeswaran S, Pohekar SD, Kousksou T. Exergy based performance evaluation of latent heat thermal storage system: A review. Renewable and Sustainable Energy Rev. 2010; 14(9): 2580–2595. doi: 10.1016/j.rser.2010.07.051

16. ANSI. Instruments and Apparatus. In: Measurement Uncertainty. American Society of Mechanical Engineers; 1985.

17. Wu S, Yan T, Kuai Z, Pan W. Thermal conductivity enhancement on phase change materials for thermal energy storage: A review. Energy Storage Mater. 2020; 25: 251–295.

18. Lane GA. Phase change materials for energy storage nucleation to prevent supercooling. Sol Energy Mater Sol Cells. 1992; 27: 135–160.

19. Wei C, Li Y, Song J, et al. Supercooling suppression and thermal conductivity enhancement of erythritol using graphite foam with ultrahigh thermal conductivity for thermal energy storage. Int. Commun Heat Mass Tranfer. 2024; 153.